Simulating Collision Probabilities of Landing Airplanes at Nontowered Airports

John F. Shortle
Yue Xie
C. H. Chen
George L. Donohue
System Engineering & Operations Research Department
George Mason University
Fairfax, VA 22030
jshortle@gmu.edu

Making greater use of smaller airports is one way that has been proposed to increase the capacity of the National Airspace System. A major difficulty is that many small airports do not have control towers, and thus capacity is severely limited during poor visibility. The authors consider a proposed system in which airplanes self-separate, so they are able to land at higher capacities without a control tower. Before such a system is implemented, it must first be shown to be safe. Safety is a difficult metric to measure and predict because accidents are so rare. Even computer simulation can be slow because of the long time to observe accidents. One methodology that has been successful in assessing aviation safety through simulation is TOPAZ (Traffic Organizer and Perturbation AnalyZer). In this study, the authors apply the methodology to assess the safety of the proposed nontowered system.

Keywords: Aviation safety, airplane collisions, rare-event simulation

1. Introduction

The National Airspace System (NAS) is predominately a hub-and-spoke network, with about 60 hub airports and a maximum capacity of about 40 million operations per year. Current forecasts predict that demand for these airports will soon exceed capacity [1–3].

Closely coupled with the issue of capacity is the issue of *safety*. Flying airplanes closer together has the potential to increase the likelihood of an accident. Thus, any increase in capacity must be accompanied by a demonstration that such an increase will be safe. As capacity increases, the *relative* safety must decrease to achieve the same *absolute* accident rate over time. In fact, the commercial accident rate has remained relatively stable over the past two decades [4, 5], but the absolute number of accidents has increased due to more operations.

In this article, we evaluate the safety of a proposed system in which airplanes land at high volume at small airports without a control tower. Evaluating the safety of a new system is difficult. First, historical data may not directly apply to the new system, so it is generally not possible to extrapolate existing data to get a safety estimate of the new system. Second, since events such as collisions are so rare (Van Es [6] estimates the rate of plane-to-plane collisions for commercial aviation between 1980 and 1999 was about 0.3 collisions per million flights), simply observing the new system does not provide a safety estimate. Finally, new systems have new safety hazards that may have not existed before. Thus, a critical part of safety analysis is understanding what these hazards are; how they interact with and influence pilot/controller behavior, airplane trajectories, and so on; and how to numerically quantify their impact on the total system safety.

One methodology that has been successful in safety analysis is the TOPAZ (Traffic Organizer and Perturbation AnalyZer) modeling methodology,[1] developed at the National Aerospace Laboratory NLR, the Netherlands [7]. The methodology provides a two-step framework for assessing safety. The first step *qualitatively* assesses safety by identifying hazards relevant to the scenario in question. The second step *quantitatively* estimates safety through simulation. By identifying critical hazards in the first step, it is possible to create a simulation model that only samples the operational space where collisions are likely. Analytical models can also be used to further improve the efficiency of simulation.

In this article, we apply the TOPAZ methodology to predict collision probabilities of landing airplanes at small airports that do not have a control tower. Making greater

SIMULATION, Vol. 80, Issue 1, January 2004 21-31

DOI: 0.1177/0037549704042028

1. In this paper, TOPAZ refers only to the overall methodology, not to any specific model, code, or data.

use of smaller airports is one way that has been proposed to increase the capacity of the NAS. In fact, it has been estimated that 98% of the people in the United States live within a 30-minute drive of a public airport [8]. Providing greater accessibility to these airports could potentially divert passengers away from major hubs, increasing overall system capacity.

Without a control tower, capacities in instrument meteorological conditions (IMC) can be as low as three landings per hour, depending on the proximity of the airport to nearby radar coverage. We consider a proposed system in which a nearby, supporting controller is responsible for the *initial* separation of airplanes entering the airspace near the airport (i.e., leaving radar coverage). The pilots, however, are responsible for self-separation after that. We specifically investigate the probability of a collision on the runway in this system. This analysis is a step in determining the potential capacity at such nontowered airports.

The article is organized as follows: section 2 reviews some existing models for estimating collision risk. In particular, we review the Reich collision model, which has been used extensively in the TOPAZ modeling methodology. Section 3 reviews some of the quantitative techniques that have been used in the TOPAZ methodology. Section 4 presents a proposed concept of operations for landing airplanes at a nontowered airport. Section 5 presents the safety model and numerical results.

2. Collision Prediction Models

This section provides background on analytical, quantitative models that have been used to estimate collision and conflict probabilities. We particularly focus on the Reich collision model since it has been used as part of the TOPAZ methodology, and we use it in our simulation analysis.

The simplest class of models are intersection-type models. In these models, one assumes that planes fly along predetermined, crossing routes, generally at constant velocities. Under these assumptions, the probability of a collision at the crossing point can be computed from the arrival rates of airplanes along each path, their velocities, and the airplane geometries. For examples of such models, see Siddiqee [9], Geisinger [10], and Barnett [11].

A similar class of models are *geometric conflict* models [e.g., 12–14]. In these models, the velocities of the airplanes are fixed as before, but their initial positions (in three dimensions) are random. Then, based on extrapolating forward in time, it is possible to geometrically describe the set of initial locations that eventually lead to a conflict between two airplanes. (A conflict occurs when two airplanes are within, say, 5 nautical miles [nmi] of each other.) Integrating the probability density of the initial positions over the conflict region gives the probability of a conflict. These models generally assume level flight with constant velocities (see Paielli and Erzberger [13] for a generalization to a nonlevel flight).

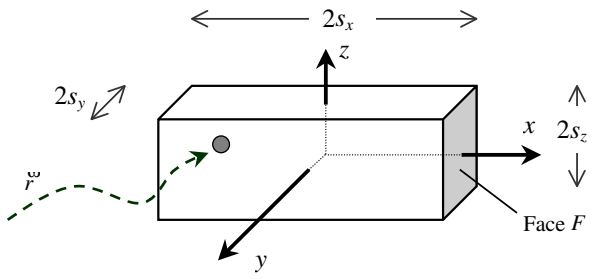

Figure 1. A geometric representation of the Reich collision model

2.1 The Reich Collision Model

A slightly more complex model is the Reich model. This model assumes random deviations in both the position and velocity components. It was originally developed to estimate collision risk for oceanic travel over the North Atlantic and to determine the appropriate spacing of flight paths [15].

To describe the model, we first start with some notation. Let $\widetilde{r}_1(t)$ and $\widetilde{v}_1(t)$ be the position and velocity vectors of one airplane at time t; let $\widetilde{r}_2(t)$ and $\widetilde{v}_2(t)$ be similarly defined for a second airplane. To simplify notation, we drop the subscript t, keeping in mind that these and related quantities have an implicit dependence on time. Let $\widetilde{r} \equiv (r_x, r_y, r_z) \equiv \widetilde{r}_1 - \widetilde{r}_2$ and $\vec{v} \equiv (v_x, v_y, v_z) \equiv \widetilde{v}_1 - \widetilde{v}_2$ be the relative position and velocity vectors of the two airplanes. Now, $\widetilde{r}$ traces out a path in time (Fig. 1). If $\widetilde{r}$ gets too small, there is a collision between the airplanes. Mathematically, if $\widetilde{r} = (0, 0, 0)$, each airplane's center of mass is at the same point in space.

The Reich model assumes that each airplane is shaped like a box, with dimensions s_x (along-track length), s_y (across-track width), and s_z (vertical height). Under these assumptions, two airplanes are touching when, for example, one airplane is in front of the other by a distance s_x or when one airplane is behind the other by a distance s_x (i.e., whenever $-s_x \le r_x \le s_x$). More generally, a collision occurs along any direction whenever $\widetilde{r}$ passes through the $2s_x \times 2s_y \times 2s_z$ box, centered at the origin in Figure 1. Such an event is called an *incrossing*.[1]

The probability of an incrossing depends on the joint probability density function (PDF) $f(\widetilde{r}, \widetilde{v}) \equiv f(r_x, r_y.r_z, v_x, v_y, v_z)$. The Reich model makes the following assumptions on this PDF:

1. The density is independent in the x, y, and z dimensions. That is,

$$f(r_x, r_y, r_z, v_x, v_y, v_z) = f_x(r_x, v_x) f_y(r_y, v_y) f_z(r_z, v_z),$$

1. Mathematically, there may be multiple incrossings. In reality, this would correspond to only one collision. Thus, the probability of an incrossing is an upper bound on the probability of a collision.

where f_x, f_y, and f_z are marginal densities of $f(\tilde{r}, \tilde{v})$.

2. The density is constant in $\tilde{r}$ over the dimensions of the aircraft. That is,

$$f_x(r_x, v_x) = f_x(0, v_x) \text{ when } |r_x| \le s_x$$

and similarly for the other dimensions. This is reasonable since the density is not expected to vary much over a distance as small as the dimensions of an airplane.[2]

3. The density is independent in the position and velocity components. That is,

$$f_x(r_x, v_x) = f_{r,x}(r_x) f_{v,x}(v_x)$$

and similarly for the other dimensions. (This assumption is not in Reich's original assumptions; however, equation (1) below, which is frequently quoted from Reich's paper [e.g., 16, 17], requires this assumption.)

Assumptions 1, 2, and 3 imply

$$f(r_x, r_y, r_z, v_x, v_y, v_z) = f_{r,x}(0) f_{r,y}(0) f_{r,z}(0)$$
$$f_{v,x}(v_x) f_{v,y}(v_y) f_{v,z}(v_z)$$

whenever $\tilde{r}$ is on or within the boundary of the collision box in Figure 1. In addition, Reich [15] assumes the following:

4. Planes travel along parallel tracks without making turns. Thus, the orientation of the collision box does not change.

5. All planes have the same geometric shape.

6. There is no evasive maneuvering by the pilot or intervention by the controller.

Under the above assumptions, the total incrossing rate through all sides of the box is

$$\varphi(t) = f_{\tilde{r}}(0, 0, 0) \sum_{i=1}^{3} A_i E|v_i|, \tag{1}$$

where the subscript i denotes the three dimensions x, y, and z; $f_{\tilde{r}}$ is the marginal density of $f(\tilde{r}, \tilde{v})$; and A_i is the area of the face perpendicular to dimension i. Also, $f_{\tilde{r}}$ and $E|v_i|$ are implicit functions of time. Since equation (1) gives the incrossing rate at time t, the total expected number of incrossings over the time interval $[a, b]$ is

$$E = \int_a^b \phi(t) dt. \tag{2}$$

2. However, if one changes the interpretation of s_x, s_y, and s_z to represent a *conflict* box (instead of a *collision* box) with dimensions of several nautical miles, then this assumption may not be valid.

If there are more than two airplanes, then equation (2) must be evaluated for every possible airplane pair and then summed to get the total number of expected incrossings among all airplanes (see equation (7) in section 5).

An advantage of the Reich collision model is that it accounts for all possible directions of the aircraft. Some of the other models, by discounting the vertical dimension, only account for collisions through the four sides of the box.

2.2 Generalized Reich Model

Some of the assumptions in the Reich model are quite restrictive—in particular, assumptions 1 and 3, which state that all components of $(\tilde{r}, \tilde{v})$ are mutually independent. In particular, velocity in one direction usually depends on velocity in another direction (e.g., the ascent rate generally depends on the along-track rate). Removing assumptions 1 and 3, Bakker and Blom [17] derived a generalized Reich collision model. In particular, the incrossing rate through a single face (face F in Fig. 1) and its opposing face is

$$\begin{aligned}\varphi_x(t) = &\int_{-s_y}^{s_y} \int_{-s_z}^{s_z} \int_{-\infty}^{0} -v_x f(v_x, r_x = s_x, r_y, r_z) dv_x dr_z dr_y \\ &+ \int_{-s_y}^{s_y} \int_{-s_z}^{s_z} \int_{0}^{\infty} v_x f(v_x, r_x = -s_x, r_y, r_z) dv_x dr_z dr_y,\end{aligned} \tag{3}$$

where $f(v_x, r_x, r_y, r_z)$ is a marginal distribution of $f(\tilde{r}, \tilde{v})$. The total incrossing rate through all faces is

$$\varphi(t) = \varphi_x(t) + \varphi_y(t) + \varphi_z(t), \tag{4}$$

where $\varphi_y(t)$ and $\varphi_z(t)$ are defined similarly to equation (3). Although equation (3) is difficult to evaluate numerically, Blom and Bakker [18] show that if $f(\tilde{r}, \tilde{v})$ is a mixture of Gaussian distributions, then evaluation of the integral is much easier.

Blom and Bakker [18] also argue that assumption 4 can be removed by assuming that $s_x = s_y$. In other words, if the length of a plane is approximately the same as its wing span, the bounding box does not change when the plane turns. That is, the collision box in Figure 1 keeps a fixed orientation, regardless of the orientation of the two airplanes.

3. Simulation Methods

The previous section discussed several analytical models to estimate collision risk. A central problem with these models is that they only apply to simple scenarios. For example, they generally apply to level flight and do not consider corrective actions by pilots or controllers. In this article, we consider the scenario of predicting plane-to-plane collisions on the runway. While relatively simple, this scenario has several complications that make the previous models by themselves insufficient. In particular, the analytical models do not account for corrective actions by

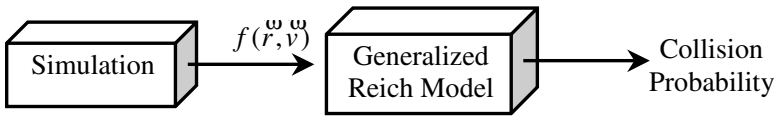

Figure 2. Basic mechanism for combining simulation with an analytical model

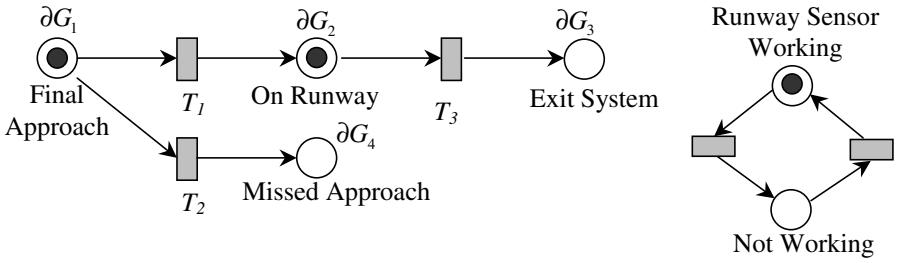

Figure 3. Simple Petri net with possible missed approach

the pilots to avoid a collision, nor do they account for equipment failures. The models, however, are still quite useful as an enhancement to simulation, as we discuss below.

We now discuss the simulation method used in several TOPAZ models to evaluate collision risk [e.g., 19]. The method uses *dynamically colored Petri nets* (DCPNs) as a framework for simulation. To improve efficiency, the method also makes use of the generalized Reich collision model, discussed in the previous section. Figure 2 shows the basic idea. Instead of returning the number of collisions, the simulation returns the probability density $f(\tilde{r}, \tilde{v})$ (the distribution for the relative position and velocity of an airplane pair). Given $f(\tilde{r}, \tilde{v})$, the probability of a collision can be calculated using the generalized Reich model, equations (3) and (4) (also see Blom and Bakker [18]).

DCPNs can simulate a wide variety of system dynamics, including flight dynamics and controller-pilot interactions. To illustrate the use of DCPNs in the context of aviation safety, we give a simple example (Fig. 3). Figure 4 gives the DCPN used to simulate the small airport application discussed in the next section. For further details on DCPNs, see Everdij, Blom, and Klompstra [20]. For an example of DCPNs applied to simultaneous approaches of two airplanes on two converging runways, see Blom, Klompstra, and Bakker [19].

Figure 3 shows two separate (but not independent) Petri nets. The right Petri net models whether a runway sensor is working. The token (solid dot) indicates the current state. The transitions (gray boxes) represent events that trigger the token to move from one state to another. In this Petri net, we suppose that times between transitions are independent random variables. For example, if they follow an exponential distribution, then the right Petri net is a continuous-time Markov chain. We can also use similar Petri nets to give a very simplified model of human cognitive states—for example, to model when a pilot is relaxed, busy, or frantic. For an example of such an application in air traffic management, see Blom, Daams, and Nijhuis [21]. Also, see Hollnagel [22] for a more complete discussion of human reliability in the context of human internal states.

The left Petri net is more mathematically complex. The tokens correspond to airplanes, and the places (open circles) correspond to phases of flight. In the figure, there is one airplane on the runway and one airplane in the final approach. Associated with each token is a six-dimensional vector (not drawn), giving the position and velocity of that airplane in three-dimensional space. Associated with each phase of flight is a set of six differential equations that govern each airplane's trajectory in time when in that phase. In the figure, ∂G_1 represents six differential equations that govern airplane trajectories in the final approach. The differential equations can be stochastic, allowing for random perturbations due to wind or pilot error. For example, two of the differential equations used in the final approach phase of the complete model (place p_{12} in Fig. 4) are as follows:

$$\begin{aligned} dp_x &= v_x dt, \\ dv_x &= -kv_x - bp_x + \sigma d\omega, \end{aligned} \tag{5}$$

where p_x and v_x are the position and velocity of the airplane in the x (across-track) dimension, $d\omega$ represents the Brownian motion, and k, b, and σ are constants. The equations represent a pilot who is trying to keep the airplane centered along the runway line (at $x = 0$) in the presence of wind. The first two terms in the second equation represent the pilot control, and the last term represents wind (i.e., in a small time interval of length Δt, the perturbation due to wind is a normal random variable with mean 0 and

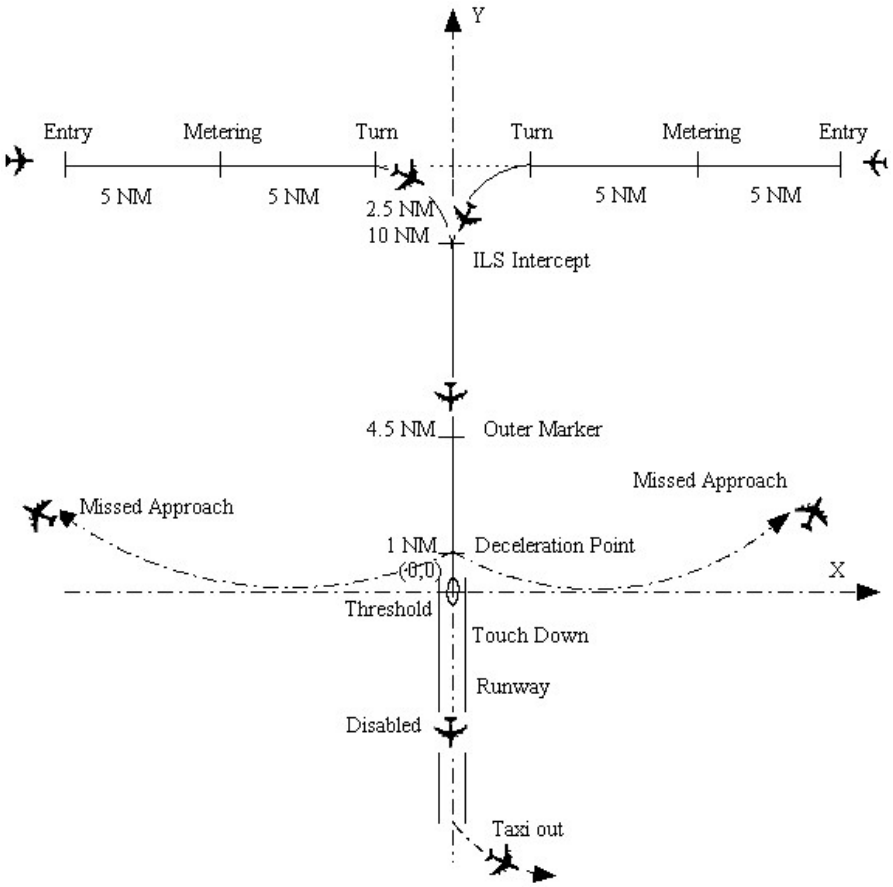

Figure 4. Airplanes landing at a small nontowered airport

variance $\sigma^2 \Delta t$). There would also be four other equations corresponding to the y and z directions. For an introduction to stochastic differential equations, see Oksendal [23].

We can also link the two Petri nets in Figure 3. For example, to model the functionality of the runway sensor, we define the transition T_1 in the left Petri net to trigger when

- the airplane in the final approach has just crossed the runway threshold (based on its position vector), *and*
- the runway is *not* occupied, *or* the runway *is* occupied but the runway sensor is not working.

Thus, the state of the right Petri net affects the trigger events of the left Petri net. This logic can also be drawn using standard Petri net notation. However, we do not do this to avoid clutter. We can also create a second type of link between the two Petri nets: making the differential equations on the left a function of the Petri net state on the right. An example would be using the right Petri net to model the state of an instrument landing system (ILS). When the ILS is not working, pilots deviate more from the glide path. Thus, two sets of differential equations are needed to model the airplane trajectory, depending on whether the ILS is working.

4. Application: Nontowered Airports

This section describes a scenario involving a small airport with no control tower. The goal is to increase the capacity of such airports in IMC. Currently, procedural separation rules dictate that only one airplane is allowed into the airspace near the airport at one time (in IMC). This "guarantees" that two airplanes are not simultaneously flying near the airport outside of radar coverage. However, this can yield capacities as low as three operations per hour depending on nearby terrain and proximity to radar coverage.

One solution that has been proposed is to equip airplanes with a self-separation capability. Nearby controllers have responsibility for the *initial* separation of airplanes into the

local airspace, but after that, airplanes must separate themselves. Referring to Figure 4, we consider the following concept of operations:

- Since the local airport does not have a control tower and is outside radar coverage, en route arrival-departure traffic is controlled by a *supporting* air traffic controller (ATCo) at a TRACON (Terminal radar approach control) or ARTCC (Air route traffic control center).
- The supporting ATCo meters airplanes into the local airspace through one of two approach legs. The two approach paths combine to form a "T." The ATCo is responsible for the initial separation of the airplanes.
- Once an airplane enters the airspace, the pilot is responsible for maintaining separation with other airplanes. At this point, the airplane is outside radar control of the ATCo.
- A small terminal sensor located on the ground at the airport provides radar-like coverage for the local airspace. The sensor fusion system transmits airplane positions to all airplanes in the local airspace via a ground-to-air data link.
- A cockpit display of traffic information (CDTI) displays the locations of these airplanes to the pilots. Pilots use the display to maintain separation.
- As a deterrent to a collision on the runway, an infrared sensor on the ground detects the presence of an airplane on the runway. If the runway is occupied, the landing pilot receives a warning in the cockpit.

Three locations where plane-to-plane collisions are most likely to occur are as follows (Fig. 4):

1. *Intersection of the "T."* The controller has not properly separated incoming airplanes.
2. *Final approach*. A faster airplane overtakes and collides with a slower airplane.
3. *Runway*. One airplane fails to exit the runway before the approaching airplane lands.

The last collision type is probably the most common. This is because there are only two degrees of freedom on the runway but three degrees of freedom in the air. Since the last collision type presents the largest safety issue, this article concentrates on that scenario. We will also discuss in the next section how the model can be used to evaluate the risk of the other collision types.

5. Analysis and Results

This section describes the analysis to estimate the probability of a collision on the runway. A first step in safety assessment is an identification of hazards (also see Blom et al. [7]). Since the focus of this article is on simulation, we do not elaborate on this step but simply list examples of hazards that can lead to a collision. Of course, the following is not an exhaustive list.

1. An airplane lands and becomes disabled, so it cannot exit the runway (blown tire, partial crash landing, etc.).
2. An airplane lands, and the pilot becomes disoriented; instead of exiting to the taxi-way, the pilot stays on the runway while going to the gate.
3. The pilot stops on the runway and does not immediately pull off.
4. The runway sensor fails.
5. The communication link between this sensor and other airborne airplanes fails.
6. The pilot fails to notice a warning from the runway sensor.
7. The pilot notices the warning but chooses to ignore it.
8. The pilot is distracted and does not see another airplane on the runway. This could be due to poor visibility or because the pilot is concentrating on landing his or her own airplane.
9. The runway is slick, so a landing airplane cannot decelerate as quickly as normal.

Figure 5 gives the Petri net structure, which models the scenario described previously. The model incorporates all of the hazards listed above. In some cases, we have grouped several hazards into a single model element. For example, the subnet in the lower left-hand corner of Figure 5 models hazards 1 through 3. The "Runway Sensor" subnet models hazards 4 and 5. The "Pilot's Awareness" subnet models hazards 6 through 8.

Table 1 gives probability estimates for hazards in the model. Since this is a proposed system, little data are available for these parameters, so at this point, they are estimates. Later in this section, we give a sensitivity analysis on these parameters to understand which parameters most affect the system safety.

To further clarify the simulation logic, if airplane i reaches the decision point (A in Fig. 6) and airplane j is disabled on the runway, then airplane i will land if the following happens (otherwise, i will fly a missed approach):

- pilot i does not receive or react to a warning from the runway sensor (due to any one of hazards 4-7), *and*
- pilot i fails to visually see airplane j while between points A and B (hazard 8).

Stochastic differential equations govern the airplane trajectory for each phase of flight. In general, these are second-order response models in which the pilot tries to maintain a target speed (different for each airplane) along a constant heading or glide slope, subject to random perturbations due to wind or pilot control.

We also make the following assumptions:

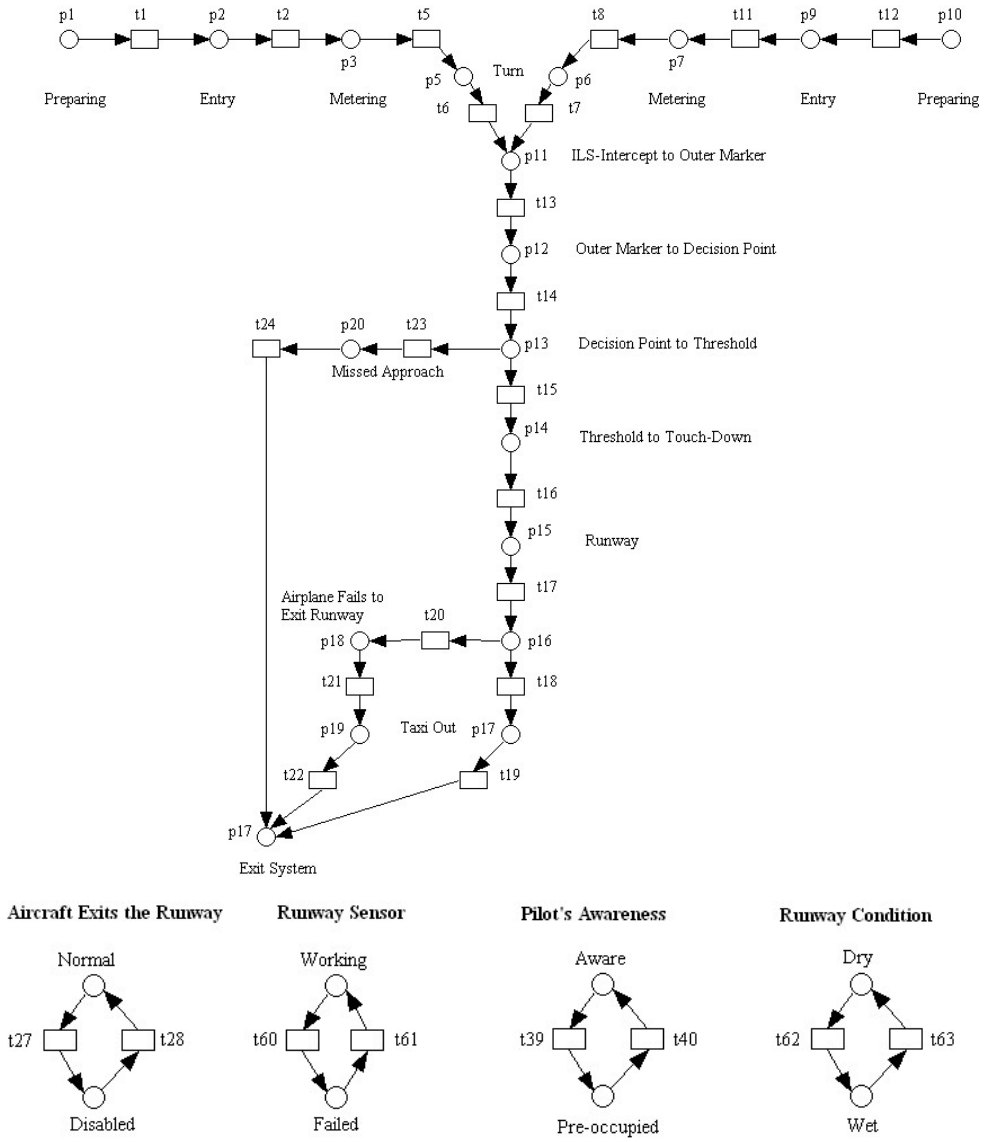

Figure 5. Petri net diagram of nontowered airport

- An airplane that fails to exit the runway remains on the runway for a random amount of time (following an exponential distribution).
- At touchdown, the pilot immediately sees a disabled airplane on the runway. At this point, the pilot decelerates the plane at the maximum possible rate.
- The runway may be wet (hazard 9) or dry. If the runway is wet, the maximum deceleration rate is less than the normal deceleration rate.

In addition, we make the following assumptions regarding weather, approach paths, and airplane types:

- Weather conditions are IMC.
- The visibility ceiling is 250 feet.
- The runway visual range is 3/4 mile.
- Pilots fly a 3-degree approach path.
- All airplanes have the same flight characteristics and onboard equipment.
- The airport has a single runway with a separate taxi-way. The runway is 5000 feet in length.

Following the methods from Blom, Klompstra, and Bakker [19], we define τ_{ij} to be a time such that there is *zero* probability of a collision between airplane i and j prior to time τ_{ij}. Since we are only interested in collisions on the runway, we can define

Table 1. Parameters used in the model

A. Landing airplane does not exit runway (hazards 1–3)	Pr(A) = 5×10^{-3}
B. Runway sensor is not working (hazards 4–5)	Pr(B) = 1×10^{-4}
C. Pilot fails to notice warning from sensor (hazards 6–7)	Pr(C) = 1×10^{-3}
D. Pilot fails to see airplane on runway (hazard 8)	Pr(D) = 1×10^{-2}
E. Runway is slick (hazard 9)	Pr(E) = 5×10^{-2}

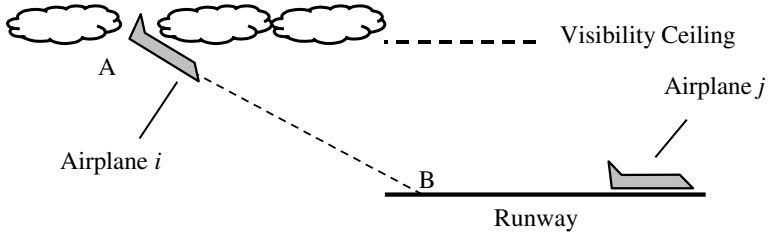

Figure 6. Airplanes landing on runway

τ_{ij} = time airplane i lands (at B in Fig. 6) while airplane j is on the runway.

We define $\tau_{ij} = \infty$ if j exits the runway before i lands, i flies a missed approach, or i lands before j. We also define

$$B_{ij} = \begin{cases} 1 & \text{if airplane } i \text{ collides with airplane } j \\ 0 & \text{otherwise} \end{cases}$$

Without loss of generality, we assume that airplanes are indexed in order of their arrival, and we only consider collisions when $i > j$ (so, $B_{ij} = 0$ for $i \leq j$). Since (by assumption) there is zero probability that airplane i collides with airplane j prior to τ_{ij}, the total probability that airplane i collides with airplane j is

$$\Pr(B_{ij} = 1) = \Pr(B_{ij} = 1 | \tau_{ij} < \infty) \Pr(\tau_{ij} < \infty). \quad (6)$$

The total expected number of collisions $E(N)$ is then

$$E(N) = \sum_{i>j} \Pr(B_{ij} = 1). \quad (7)$$

To compute the collision rate, we compute the right-hand side of equation (6). First, to evaluate $\Pr(\tau_{ij} < \infty)$, we run the simulation (Petri net in Fig. 5) and count the number of occurrences that $\tau_{ij} < \infty$ (i.e., the number of times that some airplane i lands while another airplane j is disabled on the runway).

To evaluate $\Pr(B_{ij} = 1 | \tau_{ij} < \infty)$, we first observe

$$\Pr(B_{ij} = 1 | \tau_{ij} < \infty) = \int_{\tau_{ij}}^{\infty} \varphi_{ij}(t | \tau_{ij} < \infty) dt.^{3} \quad (8)$$

To compute this, we run the simulation with parameters adjusted to achieve an artificially high number of instances where $\tau_{ij} < \infty$. In other words, we suppose that there is a very high probability that (1) airplanes become disabled on the runway and (2) pilots and sensor systems fail to observe the disabled airplane. Each time that $\tau_{ij} < \infty$, the simulation collects data on $f_t(\tilde{r}, \tilde{v})$, the relative position and velocity of the landing airplane with respect to the disabled airplane. The subscript t denotes the dependence of this density on time, where t represents the time after τ_{ij}. (In other words, $t = 0$ refers to the time when airplane i lands, while j is still on the runway.) Using the generalized Reich model, we compute $\varphi_{ij}(t | \tau_{ij} < \infty)$ using equations (3) and (4), as described in section 2. Then, we integrate as in equation (8).

Figure 7 shows the results of the preceding analysis and simulation. The figure shows the collision probability on the runway as a function of the arrival rate. The confidence intervals (95%) show potential errors due to the finite number of simulation replications.

Other sources of errors in the safety estimates include inaccuracies in parameter estimates (e.g., those in Table 1), omissions in modeling safety hazards, and simplifications in modeling system dynamics. Since this is a proposed

3. We assume here that there is a one-to-one correspondence between incrossings and collisions. This is reasonable since airplane j is stationary. Since airplane i is always moving forwards, there is no possibility of more than one incrossing.

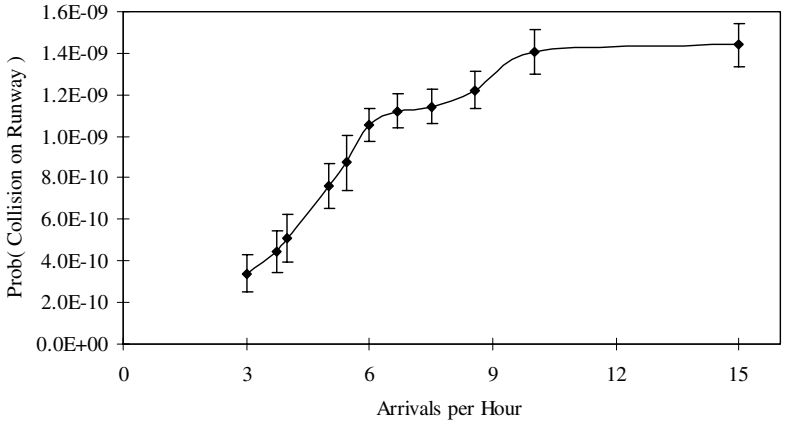

Figure 7. Collision probabilities on the runway

system and little data are available to populate some key parameters, the estimates in Figure 7, while calculated in an absolute sense, should be viewed in a relative sense. That is, the trend is more reliable than the absolute numbers.

The shape of the curve in Figure 7 is explained from the terms in equation (6). First, $\Pr(B_{ij} = 1|\tau_{ij} < \infty)$ is relatively constant as a function of the arrival rate. In other words, given that airplane i lands while airplane j is disabled on the runway, the probability of a collision does not depend much on the background arrival rate. $\Pr(\tau_{ij} < \infty)$, on the other hand, does depend on the arrival rate. As the arrival rate gets large, the probability a trailing airplane arrives (gets to point A in Fig. 6) while another airplane is on the runway levels off and goes to 1, which contributes to the basic shape in Figure 7.

Figure 8 shows sensitivity analysis for the parameters in Table 1 (under 15 arrivals per hour). From the figure, the collision probability is most sensitive to Pr(A) and Pr(D) (the two curves overlap—the reason is that A and D must both occur for a collision to occur, so a tenfold increase in Pr(A) or Pr(D) yields the same tenfold increase in the probability of a collision). The collision probability is also sensitive to Pr(C), the pilot's responsiveness to the runway warning. Therefore, from a design perspective, it is important for this sensor to be well placed in the cockpit and for the probability of a false alarm to be low, so that the pilot does not ignore the warning. An accurate estimate for the reliability of the runway sensor is not as important, nor is an accurate estimate for the probability of wet runway conditions.

While this article evaluated collisions on the runway, the same model can also be used to evaluate collisions at the top of the "T" (Fig. 4) and during the approach. The key output of the simulation is the relative separation and relative velocity PDF $f(\widetilde{r}, \widetilde{v})$ of adjacent airplanes as a function of time. For example, to estimate the probability of a collision during the approach, we can collect data from the simulation to estimate $f(\widetilde{r}, \widetilde{v})$ when airplanes are in this phase of flight. We then enter the resulting distribution into the generalized Reich collision model. A collision at the intersection presents a new challenge since the airplanes are turning. Although the Petri net model in this study provides equations of motion for the turn, we have observed that the distribution of $f(\widetilde{r}, \widetilde{v})$ in this area is not well described by a normal distribution. Since the efficient methods for integrating equations (3) and (4) in Blom and Bakker [18] require a mixture of normals, there are further numerical issues with doing this computation.

6. Conclusions

In this article, we applied the TOPAZ modeling methodology to estimate collision probabilities of airplanes landing at airports without control towers. Since collisions are rare, we used two techniques to increase the efficiency of simulation (similar to techniques used in Blom, Klompstra, and Bakker [19]): (1) conditioning on hazardous events (so the probability of a simulated collision is higher) and (2) using the generalized Reich collision model to enhance the results of simulation. Performance using these techniques was good since we were able to get statistically significant results without excessive computer time (several hours on a PC).

Of course, simulation output can only be as good as the model generating the output. In safety modeling, it is impossible to account for *all* hazards that might lead to a collision. For example, this study did not consider hazards related to improper initial separations due to controller errors. This omission biases the collision probability estimate to be lower than actual. On the other hand, some

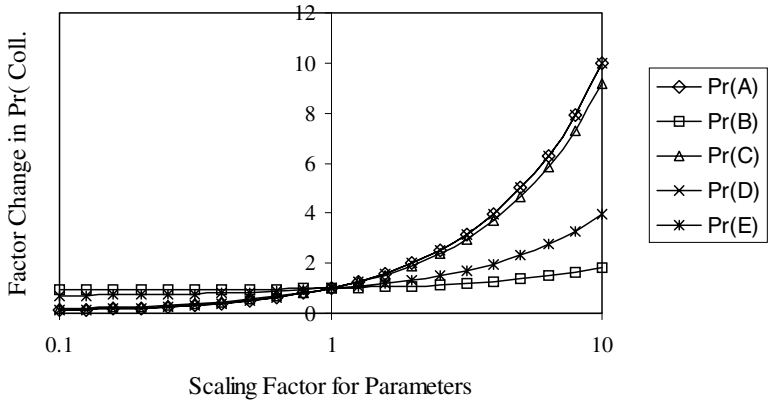

Figure 8. Sensitivity of collision probability to model parameters (the curves for Pr(A) and Pr(D) overlap)

parameter estimates are likely conservative, biasing the estimate in the other direction. Thus, conclusions based on the absolute results are tentative.

Nevertheless, we feel that such analysis has the following benefits. First, since this study considers a proposed system, the spirit is to reveal general trends. In particular, the analysis reveals a leveling off of the runway collision risk as a function of arrival rate, contrary to an expected quadratic or exponential growth. Second, the analysis identifies critical parameters that have the highest impact on safety. In this case, pilot awareness is more critical than the reliability of the runway-sensing device.

In fact, this last point illustrates a potential new use for the TOPAZ methodology. While the methodology has generally been used to evaluate the safety of *existing* air transportation systems, this study has examined a *future* system. Although initially there are little data to populate the model, we can use such a model to intelligently guide the design of data and flight tests. That is, a new system must be proven to be safe, and a critical step in this process is a demonstration of the system with real flight tests. The model can help determine what data are most important to collect and how much data should be collected in such tests. A general iterative procedure for using the TOPAZ methodology in this way is as follows: First, build a preliminary model to identify parameters that most affect safety. Then, design experiments to collect an appropriate amount of data on those parameters. Then, revise the model using the new data. These steps can be repeated until a sufficiently accurate safety estimate is achieved.

7. Acknowledgments

The authors wish to thank Henk Blom and Bert Bakker for their helpful and generous instruction in applying the TOPAZ methodology.

8. References

[1] Air Transport Action Group. 2000. European traffic forecasts 1985-2015. Accessed July 22, 2002, from http://www.atag.org/ETF/Index.htm

[2] Donohue, G. L., and R. Shaver. 2000. United States air transportation capacity: Limits to growth part I (modeling) and part II (policy). Paper presented at the 79th annual meeting of the Transportation Research Board, Papers 00-582, 00-0583, Washington, DC.

[3] EUROCONTROL. 1999-2000. Performance Review Commission, Special Performance Review Report on Delays (PRR 2) and Third Performance Review Report (PRR 3), Brussels. Retrieved from http://www.eurocontrol.be/prc/temp/prr4/reference.html

[4] Barnett, A., and M. K. Higgins. 1989. Airline safety: The last decade. *Management Science* 35 (1): 1-21.

[5] Machol, R. E. 1995. Thirty years of modeling midair collisions. *Interfaces* 25 (5): 151-72.

[6] van Es, G. W. H. 2001. A review of civil aviation accidents, air traffic management related accidents: 1980-1999. Paper presented at the 4th International Air Traffic Management R&D Seminar, December, Santa Fe, NM.

[7] Blom, H., G. J. Bakker, P. J. G. Blanker, J. Daams, M. H. C. Everdij, and M. B. Klompstra. 2001. Accident risk assessment for advanced air traffic management. In *Air transportation systems engineering*, edited by G. Donohue and A. Zellweger, 463-80. Lexington, MA: American Institute of Aeronautics and Astronautics.

[8] Holmes, B. J. 2002. Small airplanes transportation system: A vision for 21st century transportation alternatives. NASA Langley Research Center. Accessed July 23, 2002, from http://sats.nasa.gov/

[9] Siddiqee, W. 1973. A mathematical model for predicting the number of potential conflict situations at intersecting air routes. *Transportation Science* 7:158.

[10] Geisinger, K. 1985. Airspace conflict equations. *Transportation Science* 19:139-53.

[11] Barnett, A. 2000. Free-flight and en route air safety: A first-order analysis. *Operations Research* 48:833-45.

[12] Paielli, R. A., and H. Erzberger. 1997. Conflict probability estimation for free flight. *Journal of Guidance, Control, and Dynamics* 20:588-96.

[13] Paielli, R. A., and H. Erzberger. 1999. Conflict probability estimation generalized to non-level flight. *Air Traffic Control Quarterly* 7:195-222.

[14] Irvine, R. 2002. A geometrical approach to conflict probability estimation. *Air Traffic Control Quarterly* 10:85-113.

[15] Reich, P. G. 1966. Analysis of long range air traffic systems: Separation standards—I, II, and III. *Journal of the Institute of Navigation* 19:88- 96, 169-76, 331-38.
[16] Hazelrigg, G. A., and A. C. Busch. 1986. Setting navigational performance standards for aircraft flying over the oceans. *Transportation Research A* 20A:373-83.
[17] Bakker, G. J., and H. Blom. 1993. Air traffic collision risk modelling. In *32nd IEEE Conference on Decision and Control*, pp. 1464-9.
[18] Blom, H., and G. J. Bakker. 2002. Conflict probability and incrossing probability in air traffic management. In *IEEE Conference on Decision and Control*, pp. 2421-6.
[19] Blom, H., M. B. Klompstra, and G. J. Bakker. 2003. Accident risk assessment of simultaneous converging instrument approaches. *Air Traffic Control Quarterly* 11:123-55.
[20] Everdij, M. H. C., H. A. P. Blom, and M. B. Klompstra. 1997. Dynamically coloured Petri nets for air traffic management safety purposes. In *8th IFAC Symposium on Transportation Systems*, Chania, Greece, pp. 184-9.
[21] Blom, H., J. Daams, and H. B. Nijhuis. 2001. Human cognition modelling in air traffic management safety assessment. In *Air transportation systems engineering*, edited by G. Donohue and A. Zellweger, 480-512. Lexington, MA: American Institute of Aeronautics and Astronautics.
[22] Hollnagel, E. 1993. *Human reliability analysis: Context and control*. New York: Academic Press.
[23] Oksendal, B. 1992. *Stochastic differential equations: An introduction with applications*. 3d ed. New York: Springer-Verlag.

John F. Shortle *is an assistant professor in the System Engineering & Operations Research Department at George Mason University, Fairfax, Virginia.*

Yue Xie *is a doctoral candidate in the System Engineering & Operations Research Department at George Mason University, Fairfax, Virginia.*

C. H. Chen *is an associate professor in the System Engineering & Operations Research Department at George Mason University, Fairfax, Virginia.*

George L. Donohue *is a professor in the System Engineering & Operations Research Department at George Mason University, Fairfax, Virginia.*